

A multiscale method for analysis of heterogeneous thin slabs with irreducible three dimensional microstructures

Dongdong Wang* and Lingming Fang

Department of Civil Engineering, Xiamen University, Xiamen, Fujian, 361005, China

(Received July 9, 2010, Accepted August 17, 2010)

Abstract. A multiscale method is presented for analysis of thin slab structures in which the microstructures can not be reduced to two-dimensional plane stress models and thus three dimensional treatment of microstructures is necessary. This method is based on the classical asymptotic expansion multiscale approach but with consideration of the special geometric characteristics of the slab structures. This is achieved via a special form of multiscale asymptotic expansion of displacement field. The expanded three dimensional displacement field only exhibits in-plane periodicity and the thickness dimension is in the global scale. Consequently by employing the multiscale asymptotic expansion approach the global macroscopic structural problem and the local microscopic unit cell problem are rationally set up. It is noted that the unit cell is subjected to the in-plane periodic boundary conditions as well as the traction free conditions on the out of plane surfaces of the unit cell. The variational formulation and finite element implementation of the unit cell problem are discussed in details. Thereafter the in-plane material response is systematically characterized via homogenization analysis of the proposed special unit cell problem for different microstructures and the reasoning of the present method is justified. Moreover the present multiscale analysis procedure is illustrated through a plane stress beam example.

Keywords: slab structure; multiscale method; asymptotic expansion; unit cell, homogenization.

1. Introduction

Thin heterogeneous slab structures such as fiber reinforced plates are commonly employed in engineering practice. Due to the fact of the distinct ratio between the in-plane and out of plane dimensions of this type of structures it is quite reasonable to efficiently analyze these problems based on the conventional plane stress condition when in-plane loads are considered. However because of the significant scale difference between the local microstructures and global structures it is not practical to model the structures simultaneously with local and global details. On the other hand for heterogeneous slab structures the in-plane material response may be obtained first through a homogenization procedure and then the global analysis is carried out under the plane stress circumstance. For analytical homogenization methods it is often difficult to consider the interaction between the inclusions (Mura 1987, Nemat-Nasser and Hori 1993), while the rapidly developed computational multiscale analysis methods provide a very robust way to obtain the homogenized

* Corresponding author, Professor, E-mail: ddwang@xmu.edu.cn

material properties for efficient global structural analysis and meanwhile the desired detailed local information can also be extracted conveniently (Sanchez-Palebnica and Zaoui 1987, Ponte Castaneda and Suquet 1998, Hassani and Hinton 1998, Mang *et al.* 2009).

Among the various existing computational homogenization methods, the asymptotic expansion method (Bensoussan *et al.* 1978) offers a rational multiscale framework to carry out the homogenization analysis as well as the localization analysis. Consequently the asymptotic expansion method has received considerable research attention and wide applications. An adaptive finite element homogenization analysis was introduced for composite materials by Guedes and Kikuchi (1989). Swan (1994) presented the stress- and strain-controlled homogenization methods in a very systematic manner. Fish *et al.* (1997) analyzed plasticity of composites by employing the method of asymptotic expansion homogenization. The asymptotic expansion method was also used to complete multiple scale model reduction by Yuan and Fish (2009). Ghosh and Moorthy (1995) and Ghosh *et al.* (2009) combined the voronoi cell finite element method and asymptotic expansion method to formulate the multiscale analysis of elastic-plastic and ductile fracture problems. Takano *et al.* (2000) developed a large deformation asymptotic expansion formulation for composites and the micro-to-macro scale transitions was discussed by Miehe and Koch (2002) and Kaczmarczyk *et al.* (2008). Cao *et al.* (2002) presented a multiscale asymptotic analysis and numerical simulation for the second order Helmholtz equation with oscillating coefficients. Chung and Namburu (2003) also proposed an asymptotic expansion formulation for multiscale atomistic-continuum homogenization. Chen and Mehraeen (2004, 2005) developed a variationally consistent multiscale asymptotic expansion method for modeling stressed grain growth. Zhang *et al.* (2006) proposed a total Lagrangian multiscale formulation to analyze dislocation-induced plastic deformation in polycrystalline materials. The thermo-mechanical analysis of periodic multiphase materials using asymptotic expansion multiscale method was discussed by Zhang *et al.* (2006). Han *et al.* (2008) proposed a statistical two-order and two-scale method for predicting the mechanics parameters of core-shell particle-filled polymer composites. Moreover an iterative asymptotic expansion method for elliptic eigenvalue problems with oscillating coefficients was presented by Mehraeen *et al.* (2009). In the context of meshfree methods, Wang *et al.* (2003) developed an enriched interface meshfree method for large deformation homogenization analysis of magnetostrictive particle-filled elastomers. More recently Wu and Koishi (2009) introduced a meshfree procedure for the microscopic analysis of particle-reinforced rubber compounds. A comprehensive review of multiscale asymptotic expansion methods may be found from the recent monograph edited by Fish (2008).

The aforementioned works mainly concern three dimensional or two dimensional plane strain/ plane stress continuum problems. In this work the slab structure as shown in Fig. 1 is considered. This type of structure only exhibits the in-plane periodicity and along the thickness direction there are the traction free boundary conditions on the upper and bottom surfaces. It is noted although in the global scale the slab can be treated as a plane stress state while in the local scale the microstructure like the unit cell is completely three dimensional and consequently the local problem can not be reasonably modeled under either plane stress or plane strain conditions which were well discussed in existing literature (Hassani and Hinton 1998). Furthermore even the three dimensional asymptotic multiscale modeling is also problematic since there is no periodicity in the thickness direction and actually the thickness coordinate is in the global scale. Thus a consistent asymptotic expansion multiscale method is necessary for this class of structures. In this study a special form of asymptotic expansion is proposed for the asymptotic expression of displacement field. Subsequently within the multiscale expansion framework the governing equations at macroscale and microscale

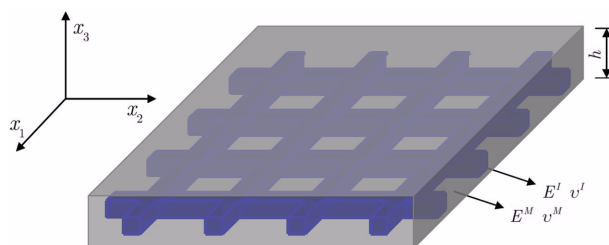


Fig. 1 A slab structure with three dimensional heterogeneities

are derived consistently and rationally. This formulation fully incorporates the in-plane periodicity characteristic and free surface boundary conditions of the unit cell. Several typical examples are considered to validate the proposed method.

The layout of this paper is as follows. The formulation of the proposed multiscale method is presented in section 2. In section 3 the variational formulation of the proposed unit cell problem and its finite element discretization are discussed. Subsequently in section 4 the algorithm verification and homogenization analyses are performed for various slab microstructures and the multiscale procedure is illustrated through a cantilever beam problem. Finally conclusions are drawn in section 5.

2. Multiscale formulation for slab structure

2.1 Asymptotic expansion of displacement field

In multiscale analysis the length scales associated with the macroscopic and microscopic material behaviors need to be considered. Let's denote the local (microscopic) coordinate system by $y = \{y_i\}_{i=1}^3$ and global (macroscopic) coordinate system by $x = \{x_i\}_{i=1}^3$ which are shown in Figs. 1 and 2, respectively. For convenience the planes of y_1y_2 and x_1x_2 are set to be the mid-plane of the slab, while y_3 and x_3 denote the thickness direction. Thus for the slab structure considered herein, the local and global coordinates are related as

$$\begin{cases} \varepsilon = \frac{x_\alpha}{y_\alpha} \ll 1, \alpha = \{1, 2\} \\ x_3 = y_3 \end{cases} \quad (1)$$

where ε is a very small positive real number. It is noted that since the periodicity only occurs in the in-plane dimensions and thus the out of plane direction, i.e., y_3 , is kept at the global scale, or there are no distinction between the global and local scales in the thickness direction, say, $x_3 = y_3$.

According to the multiscale theory by asymptotic expansion method (Bensoussan *et al.* 1978, Hassani and Hinton 1998), the homogenization and localization process can be carried out within a representative volume element, or a unit cell. As shown in Fig. 2 the definition of a unit cell is not unique, i.e., unit cells I and II both are properly defined unit cells of the slab structure as shown in Fig. 1. Here a unit cell of microstructure can be defined as

$$\Omega_y = (0, \lambda_1) \otimes (0, \lambda_2) \otimes (-h/2, h/2) \quad (2)$$

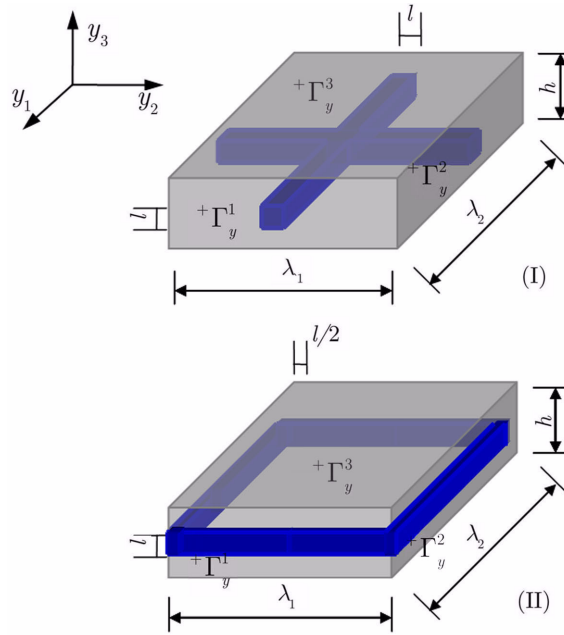


Fig. 2 Notations for unit cells

where λ_1 and λ_2 denote the in-plane y_1 and y_2 dimensions of the unit cell and h is the thickness of the slab. It is noted that the unit cell $\Omega_y = \Omega_y^I \cup \Omega_y^M$ and Ω_y^I and Ω_y^M denote the material domains of inclusion and matrix, respectively. The boundary of the unit cell, i.e. Γ_y , is the union of three surface pairs $\{^+\Gamma_y^i, ^-\Gamma_y^i\}_{i=1}^3$ in each y_i -direction as shown in Fig. 2.

To represent the in-plane only periodicity relationship, herein the following asymptotic expansion of displacement field is proposed

$$u_k^\varepsilon(\mathbf{x}) = u_k(x_\omega, y_\omega, y_3) = u_k^0(x_\omega, y_\omega, y_3) + \varepsilon u_k^1\left(x_\omega, y_\omega, \frac{y_3}{\varepsilon}\right); \quad \alpha = \{1, 2\}, k = \{1, 2, 3\} \quad (3)$$

where for brevity only first order expansion is considered without loss of generality. Thus according to Eqs. (1) and (3), one has

$$\frac{\partial u_k^\varepsilon(\mathbf{x})}{\partial x_3} = \frac{\partial u_k^\varepsilon(\mathbf{x})}{\partial y_3} = \frac{\partial u_k^0(x_\omega, y_\omega, y_3)}{\partial y_3} + \varepsilon \frac{\partial u_k^1\left(x_\omega, y_\omega, \frac{y_3}{\varepsilon}\right)}{\partial y_3} = \frac{\partial u_k^0(x_\omega, y_\omega, y_3)}{\partial y_3} + \frac{\partial u_k^1(x_\omega, y_\omega, y_3)}{\partial y_3} \quad (4)$$

where the following relationship is used

$$\frac{\partial u_k^1\left(x_\omega, y_\omega, \frac{y_3}{\varepsilon}\right)}{\partial y_3} = \frac{1}{\varepsilon} \frac{\partial u_k^1(x_\omega, y_\omega, y_3)}{\partial y_3} \quad (5)$$

Eq. (5) is exact in case that the fluctuating displacement u_k^1 varies linearly with the thickness coordinate y_3 and this is a very reasonable hypothesis for slab or plate structures. It is also noted

that Eq. (4) states that the gradient of a displacement component u_k^ε with respect to the thickness coordinate y_3 all falls into the global scale, which perfectly represents the physical periodicity happens only in the y_1 and y_2 directions.

Moreover from Eq. (1), one knows that if a function $\phi^\varepsilon(\mathbf{x})$ depends on both the local and global coordinates, i.e., $\phi^\varepsilon(\mathbf{x}) = \phi(\mathbf{x}, \mathbf{y})$, the following relationship holds

$$\frac{\partial \phi^\varepsilon(\mathbf{x})}{\partial x_\alpha} = \frac{\partial \phi(\mathbf{x}, \mathbf{y})}{\partial x_\alpha} = \frac{\partial \phi}{\partial x_\alpha} + \frac{1}{\varepsilon} \frac{\partial \phi}{\partial y_\alpha}; \quad \alpha = \{1, 2\} \quad (6)$$

Subsequently by using Eqs. (4) and (6) the following equations of displacement gradients can be readily obtained

$$\begin{cases} \frac{\partial u_k^\varepsilon}{\partial x_\beta} = \frac{1}{\varepsilon} \frac{\partial u_k^0}{\partial y_\beta} + \left(\frac{\partial u_k^0}{\partial x_\beta} + \frac{\partial u_k^1}{\partial y_\beta} \right) + \varepsilon \frac{\partial u_k^1}{\partial x_\beta}; & \beta = \{1, 2\} \\ \frac{\partial u_k^\varepsilon}{\partial x_3} = \frac{\partial u_k^0}{\partial y_3} + \frac{\partial u_k^1}{\partial y_3} \end{cases} \quad (7)$$

2.2 Derivation of local and global problems

The local and global problems can be rationally derived from the three dimensional equilibrium equation of heterogeneous media

$$\frac{\partial \sigma_{ij}^\varepsilon}{\partial x_j} = 0; \quad \{i, j\} = \{1, 2, 3\} \quad (8)$$

where σ_{ij}^ε denotes the stress tensor and the body force is ignored. The constitutive relationship is given by

$$\sigma_{ij}^\varepsilon = C_{ijkl} \frac{\partial u_k^\varepsilon}{\partial x_l} \quad (9)$$

with C_{ijkl} being the fourth order elasticity tensor.

Substituting Eq. (7) into Eq. (9) yields

$$\begin{aligned} \sigma_{ij}^\varepsilon = C_{ijkl} \frac{\partial u_k^\varepsilon}{\partial x_l} &= C_{ijk\beta} \frac{\partial u_k^\varepsilon}{\partial x_\beta} + C_{ijk3} \frac{\partial u_k^\varepsilon}{\partial x_3} = \frac{1}{\varepsilon} \sigma_{ij}^{-1} + \sigma_{ij} + \varepsilon \sigma_{ij}^1; \\ \beta = \{1, 2\}, \{i, j, k, l\} &= \{1, 2, 3\} \end{aligned} \quad (10)$$

where σ_{ij}^{-1} , σ_{ij} and σ_{ij}^1 are defined by

$$\sigma_{ij}^{-1} = C_{ijk\beta} \frac{\partial u_k^0}{\partial y_\beta} \quad (11)$$

$$\sigma_{ij} = C_{ijkl} \left(\frac{\partial u_k^0}{\partial x_l} + \frac{\partial u_k^1}{\partial y_l} \right) \quad (12)$$

$$\sigma_{ij}^1 = C_{ijk\beta} \frac{\partial u_k^1}{\partial x_\beta} \quad (13)$$

Further plugging Eq. (10) into Eq. (8) gives

$$\frac{1}{\varepsilon^2} \frac{\partial \sigma_{i\alpha}^{-1}}{\partial y_\alpha} + \frac{1}{\varepsilon} \left(\frac{\partial \sigma_{ij}^{-1}}{\partial x_j} + \frac{\partial \sigma_{ij}}{\partial y_j} \right) + \left(\frac{\partial \sigma_{i\alpha}}{\partial x_\alpha} + \frac{\partial \sigma_{ij}^1}{\partial y_j} \right) = 0; \quad \alpha = \{1, 2\}, \{i, j\} = \{1, 2, 3\} \quad (14)$$

Due to the fact of $\varepsilon \ll 1$, Eq. (14) implies the following three equations

$$\frac{\partial \sigma_{i\alpha}^{-1}}{\partial y_\alpha} = 0; \quad \alpha = \{1, 2\}, i = \{1, 2, 3\} \quad (15)$$

$$\frac{\partial \sigma_{ij}^{-1}}{\partial x_j} + \frac{\partial \sigma_{ij}}{\partial y_j} = 0; \quad \{i, j\} = \{1, 2, 3\} \quad (16)$$

$$\frac{\partial \sigma_{i\alpha}}{\partial x_\alpha} + \frac{\partial \sigma_{ij}^1}{\partial y_j} = 0; \quad \alpha = \{1, 2\}, \{i, j\} = \{1, 2, 3\} \quad (17)$$

From the positive definite property of the elasticity tensor and by using Eq. (11), Eq. (15) yields

$$\begin{cases} u_k^0(\mathbf{x}, \mathbf{y}) = u_k^0(\mathbf{x}) \\ \sigma_{ij}^{-1} = 0 \end{cases} \quad (18)$$

Moreover, through substitution of Eq. (18) into Eq. (16) the local unit cell problem can be obtained

$$\frac{\partial \sigma_{ij}}{\partial y_j} = 0 \quad (19)$$

This unit cell problem is subjected to the periodic boundary conditions on the surrounding surfaces

$$(u_i - \bar{u}_i)|_{\Gamma_y^\alpha} = (u_i - \bar{u}_i)|_{\Gamma_y^\alpha} \quad (20)$$

and the traction free boundary conditions on the upper and lower surfaces

$$t_i = \sigma_{ij} n_j = 0 \quad \text{on} \quad {}^+ \Gamma_y^3 \cup {}^- \Gamma_y^3 \quad (21)$$

with n_j being the outward surface normal of the corresponding upper and lower surfaces. \bar{u}_i in Eq. (20) represents the displacement of a specific reference material point, i.e., the surface centroid, on the surrounding surfaces $\{{}^+ \Gamma_y^\alpha, {}^- \Gamma_y^\alpha\}_{\alpha=1}^2$. Consequently the periodicity condition of Eq. (20) reduces to the following constraints on the fluctuating displacement \mathbf{u}^1

$$u_i^1|_{\Gamma_y^\alpha} = u_i^1|_{\Gamma_y^\alpha} \quad (22)$$

Finally a volume average of Eq. (17) over the unit cell gives the global equilibrium equation

$$\frac{\partial \langle \sigma_{i\alpha} \rangle}{\partial x_\alpha} = 0 \quad (23)$$

where $\langle \bullet \rangle = (\Omega_y^{-1}) \int_{\Omega_y} (\bullet) d\Omega$ and the periodic properties and free boundary conditions over the upper and bottom unit cell surfaces is made for σ_{ij}^1 . For $i = 1, 2$, Eq. (23) produces the in-plane global equilibrium equations corresponding to a plane stress state, while for $i = 3$, Eq. (23) gives the transverse equilibrium over the thickness of the slab structure.

3. Variational formulation and discretization of local problem

The variational form corresponding to the local unit cell problem of Eq. (19) can be stated as

$$\int_{\Omega_y} \delta u_i^1 \frac{\partial \sigma_{ij}}{\partial y_j} d\Omega = 0 \quad (24)$$

with δu_i^1 denoting the virtual displacement. After the operation of integration by parts, Eq. (24) becomes

$$\int_{\Omega_y} \frac{\partial \delta u_i^1}{\partial y_j} \sigma_{ij} d\Omega = \int_{\Gamma_y} \delta u_i^1 t_i dS = 0 \quad (25)$$

where use is made of the following relationship

$$\int_{\Gamma_y} \delta u_i^1 t_i d\Omega = \int_{\Gamma_y^3 \cup -\Gamma_y^3} \delta u_i^1 \underbrace{t_i}_{= 0(\text{traction free})} dS + \underbrace{\int_{\Gamma_y^\alpha \cup -\Gamma_y^\alpha} \delta u_i^1 t_i dS}_{= 0(\text{periodicity})} = 0 \quad (26)$$

Note here the traction free boundary conditions on the upper and lower surfaces are embedded into the present formulation. Further substitution of Eq. (12) into Eq. (25) gives

$$\int_{\Omega_y} \frac{\partial \delta u_i^1}{\partial y_j} C_{ijkl} \frac{\partial u_k^1}{\partial y_l} d\Omega = - \int_{\Omega_y} \frac{\partial \delta u_i^1}{\partial y_j} C_{ijkl} \frac{\partial u_k^0}{\partial x_l} d\Omega \quad (27)$$

For convenience of development, the following matrix-vector notations are defined

$$\begin{cases} \bar{\boldsymbol{\varepsilon}} = \left[\frac{\partial u_1^0}{\partial x_1} \frac{\partial u_2^0}{\partial x_2} \frac{\partial u_3^0}{\partial x_3} \frac{\partial u_1^0}{\partial x_2} + \frac{\partial u_2^0}{\partial x_1} \frac{\partial u_1^0}{\partial x_3} + \frac{\partial u_3^0}{\partial x_1} \frac{\partial u_2^0}{\partial x_3} + \frac{\partial u_3^0}{\partial x_2} \right]^T \\ \delta \mathbf{u}^* = [\delta u_1^1 \ \delta u_2^1 \ \delta u_3^1]^T \\ \mathbf{u}^* = [u_1^1 \ u_2^1 \ u_3^1]^T \end{cases} \quad (28)$$

$$\mathcal{L} = \begin{bmatrix} \frac{\partial}{\partial y_1} & 0 & 0 \\ 0 & \frac{\partial}{\partial y_2} & 0 \\ 0 & 0 & \frac{\partial}{\partial y_3} \\ \frac{\partial}{\partial y_2} & \frac{\partial}{\partial y_1} & 0 \\ \frac{\partial}{\partial y_3} & 0 & \frac{\partial}{\partial y_1} \\ 0 & \frac{\partial}{\partial y_3} & \frac{\partial}{\partial y_2} \end{bmatrix} \quad (29)$$

$$\mathbf{D} = \begin{bmatrix} C_{1111} & C_{1122} & C_{1133} & C_{1112} & C_{1113} & C_{1123} \\ C_{2211} & C_{2222} & C_{2233} & C_{2212} & C_{2213} & C_{2223} \\ C_{3311} & C_{3322} & C_{3333} & C_{3312} & C_{3313} & C_{3323} \\ C_{1211} & C_{1222} & C_{1233} & C_{1212} & C_{1213} & C_{1223} \\ C_{1311} & C_{1322} & C_{1333} & C_{1312} & C_{1313} & C_{1323} \\ C_{2311} & C_{2322} & C_{2333} & C_{2312} & C_{2313} & C_{2323} \end{bmatrix} \quad (30)$$

With Eqs. (28)-(30), Eq. (27) can be rewritten as

$$\int_{\Omega_y} (\mathcal{L}(\delta \mathbf{u}^*))^T \mathbf{D} (\mathcal{L} \mathbf{u}^*) d\Omega = - \int_{\Omega_y} (\mathcal{L}(\delta \mathbf{u}^*))^T \mathbf{D} \bar{\boldsymbol{\varepsilon}} d\Omega \quad (31)$$

Introducing a standard finite element approximation with the three dimensional eight-node hexahedral elements

$$\mathbf{u}^* = \sum_{A=1}^{n_{en}} N_A \mathbf{d}_A; \quad \delta \mathbf{u}^* = \sum_{A=1}^{n_{en}} N_A \delta \mathbf{d}_A \quad (32)$$

where N_A 's, $A = 1, 2, \dots, 8$, are the conventional tri-linear shape functions (Hughes 2000), n_{en} denotes the total number of nodes in an element.

Substituting Eq. (32) yields the discrete unit cell problem

$$\mathbf{K} \mathbf{d} = \mathbf{f} \quad (33)$$

with

$$\mathbf{K} = \mathcal{A} \left(\mathbf{K}^e \right); \quad \mathbf{f} = \mathcal{A} \left(\mathbf{f}^e \right) \quad (34)$$

$$\mathbf{K}_{AB}^e = \int_{\Omega^e} \mathbf{B}_A^T \mathbf{D} \mathbf{B}_B d\Omega; \quad \mathbf{f}_A^e = - \int_{\Omega^e} \mathbf{B}_A^T \mathbf{D} \bar{\boldsymbol{\varepsilon}} d\Omega; \quad \mathbf{B}_A = \mathcal{L}(N_A) \quad (35)$$

where n_{el} being the number of elements. \mathcal{A} is the standard element assembly operator (Hughes 2000). Eq. (33) is subjected to the periodic boundary conditions on the surrounding surfaces as discussed in Eq. (22) and it is also noted that the free surface conditions have been automatically satisfied as a prior in this formulation.

Thereafter to characterize the overall in-plane material response, the following three macroscopic averaged strain vectors are selected

$$\begin{cases} \bar{\boldsymbol{\varepsilon}}^{[t1]} = [1 \ 0 \ 0 \ 0 \ 0 \ 0]^T \\ \bar{\boldsymbol{\varepsilon}}^{[t2]} = [0 \ 1 \ 0 \ 0 \ 0 \ 0]^T \\ \bar{\boldsymbol{\varepsilon}}^{[s]} = [0 \ 0 \ 0 \ 1 \ 0 \ 0]^T \end{cases} \quad (36)$$

in which $\bar{\boldsymbol{\varepsilon}}^{[t1]}$ and $\bar{\boldsymbol{\varepsilon}}^{[t2]}$ represent the tension modes in y_1 and y_2 directions and $\bar{\boldsymbol{\varepsilon}}^{[s]}$ denotes the in-

plane shear mode. Subsequently one can solve the averaged stress field from the local problem of Eq. (33) and obtain the macroscopic effective in-plane material properties

$$\mathbf{D}^{eff} = \begin{bmatrix} D_{11}^{eff} & D_{12}^{eff} & D_{13}^{eff} \\ D_{21}^{eff} & D_{22}^{eff} & D_{23}^{eff} \\ D_{31}^{eff} & D_{32}^{eff} & D_{33}^{eff} \end{bmatrix} \quad (37)$$

Remarks: The unit cell analysis discussed here can be combined with the conventional global structural analysis to perform multiscale analysis. The global analysis is carried out by using the standard finite element procedure based on the macroscopic equilibrium equation of (23) and the homogenized material properties in Eq. (37), subsequently the macroscopic strain fields at given positions can be passed into the unit cell to get the desired local information.

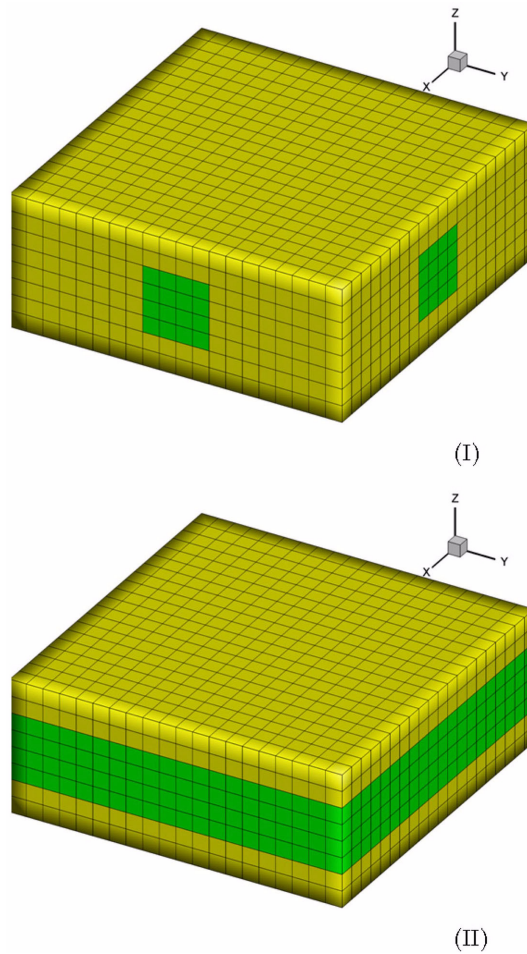


Fig. 3 Finite element discretizations for unit cells

4. Numerical examples

4.1 Algorithm verification for homogeneous slab

To verify the proposed method, a homogeneous slab structure with the unit cell as shown in Figs. 1 and 2 is first considered. The material and geometry properties for this problem are: $E^M = E^I = 10$ GPa, $\lambda_1 = \lambda_2 = 0.2$ m, $h = 0.08$ m, $l = 0.04$ m, and the Poisson's ratio for both materials is $\nu^M = \nu^I = 0.3$. Here the unit cell problem is analyzed to obtain the homogenized material properties. Obviously the homogenized material constants for this problem should follow the plane stress constitutive relationship. In this analysis the unit cells are discretized with $20 \times 20 \times 8$ conventional eight-node tri-linear finite elements that are depicted in Fig. 3. The fluctuating and total microscopic deformations of the unit cells are plotted in Figs. 4-6, which are obtained via three strain-controlled analyses corresponding to the three deformation modes defined in Eq. (36). It is noted that as expected the results show no difference between the unit cells I and II in this case. The resulting homogenized material properties are obtained as

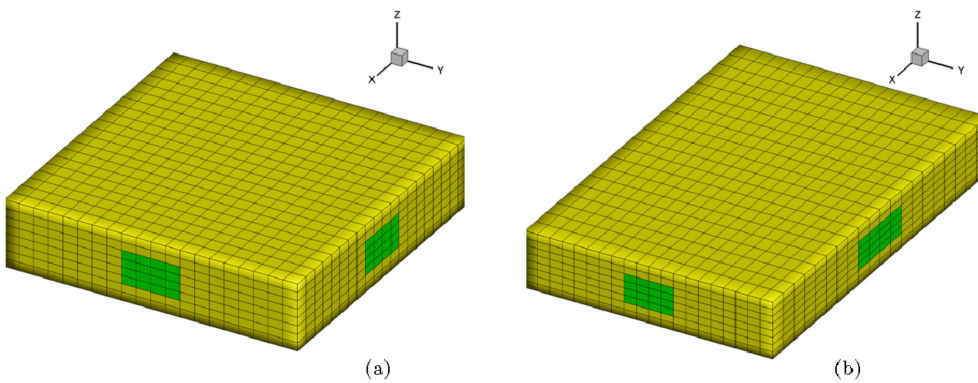


Fig. 4 Microscopic y_1 -tension deformations for homogenous material: (a) local fluctuating deformation, (b) total deformation

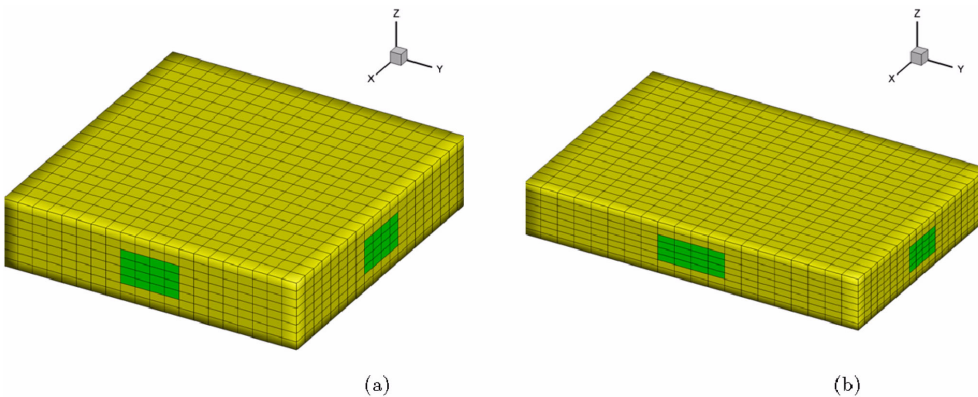


Fig. 5 Microscopic y_2 -tension deformations for homogenous material: (a) local fluctuating deformation, (b) total deformation

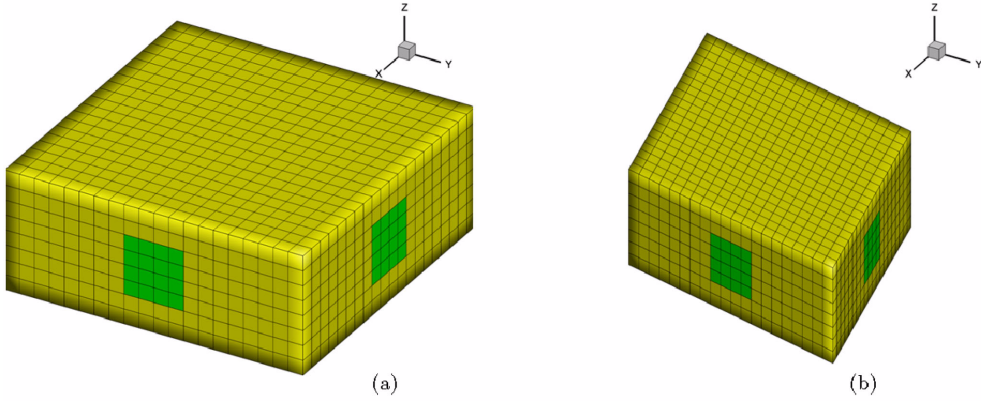


Fig. 6 Microscopic in-plane shear deformations for homogenous material: (a) local fluctuating deformation, (b) total deformation

$$\mathbf{D}^{eff} = \begin{bmatrix} 1.0989 & 0.3297 & 0 \\ 0.3297 & 1.0989 & 0 \\ 0 & 0 & 0.3846 \end{bmatrix} \times 10GPa = \frac{E}{1-\nu^2} \begin{bmatrix} 1 & \nu & 0 \\ \nu & 1 & 0 \\ 0 & 0 & (1-\nu)/2 \end{bmatrix} \quad (38)$$

Clearly the proposed method perfectly reproduces the analytical expressions for homogeneous plane stress constitutive relationship.

4.2 Homogenization analysis for heterogeneous slab

The heterogeneous slab structure as shown in Fig. 1 is again considered. The geometric information of the unit cells for this problem is the same as the previous example while the material properties for the matrix and inclusion are: $E^M = 10GPa$, $E^I = 100GPa$, $\nu^M = \nu^I = 0.3$. The corresponding volume fraction is 18%. The unit cells are also shown in Fig. 2 which have the finite element partition listed in Fig. 3. The microscopic fluctuating and total deformations of the unit cell I resulting from the prescribed in-plane tension and shear modes given in Eq. (36) are depicted in Figs. 7-9, respectively. From the local fluctuating deformations of Figs. 7-9 it can be clearly seen that the periodic characteristics of local fluctuating deformation occurs on the surrounding surfaces. The computed homogenized material properties are

$$\mathbf{D}_{(I)}^{eff} = \begin{bmatrix} 2.1880 & 0.4861 & 0.0000 \\ 0.4861 & 2.1880 & 0.0000 \\ 0.0000 & 0.0000 & 0.5430 \end{bmatrix} \times 10GPa \quad (39)$$

Moreover to examine the fact that the homogenized material properties are independent on the choice of unit cells, the unit cell II as shown in Figs. 2 and 3 is also selected for homogenization analysis. The corresponding local fluctuating deformations and the total deformations are plotted in Figs. 10-12. The homogenized material constants are exactly the same as those in Eq. (39), i.e., $\mathbf{D}_{(I)}^{eff} = \mathbf{D}_{(II)}^{eff}$. This confirms the fact that for different choice of unit cells gives no influence on the homogenized material constants although the respective local fluctuating deformations are different.

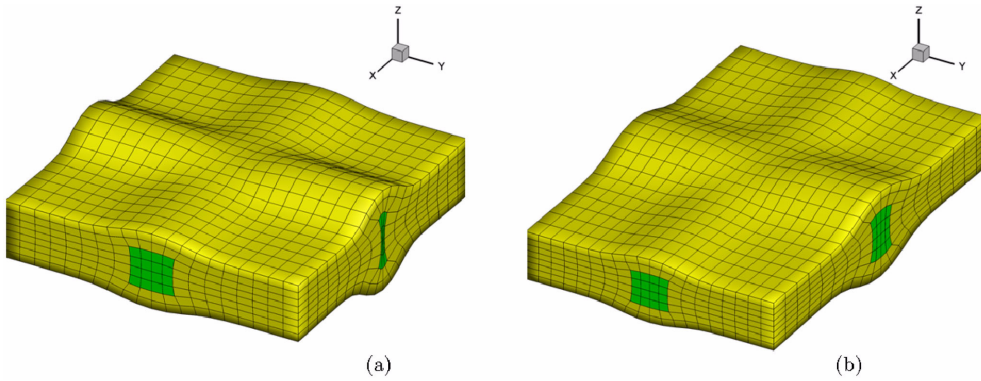


Fig. 7 Microscopic y_1 -tension deformations for unit cell I: (a) local fluctuating deformation, (b) total deformation

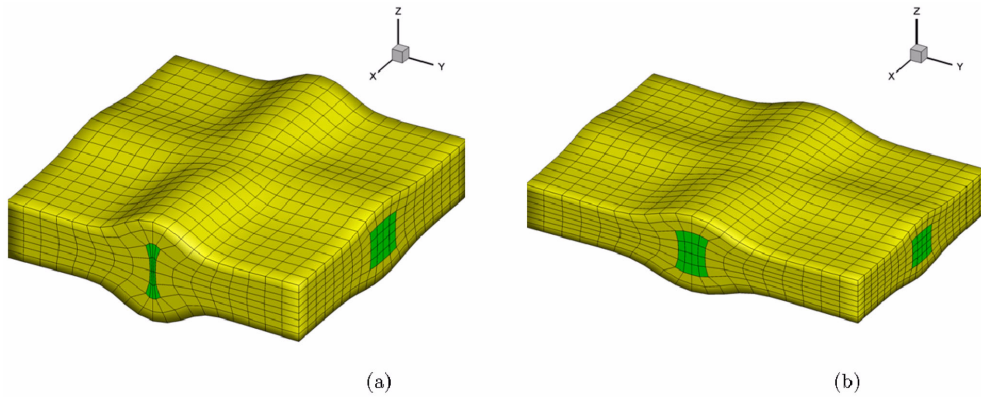


Fig. 8 Microscopic y_2 -tension deformations for unit cell I: (a) local fluctuating deformation, (b) total deformation

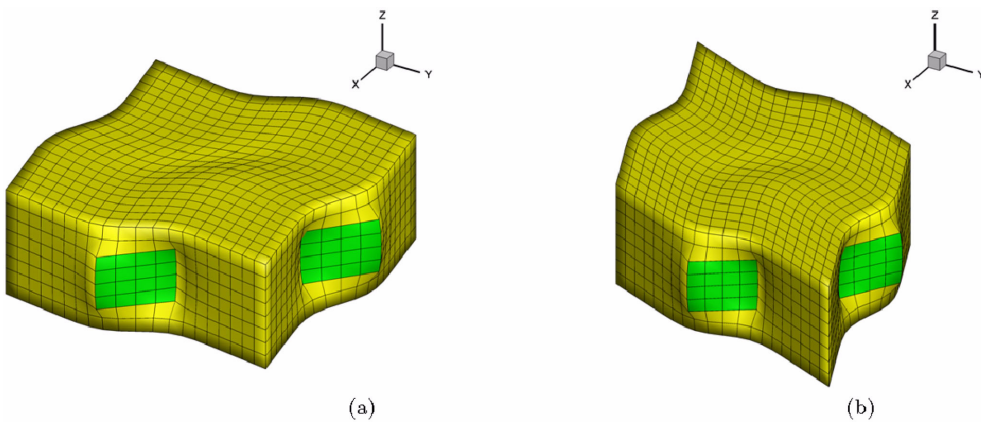


Fig. 9 Microscopic in-plane shear deformations for unit cell I: (a) local fluctuating deformation, (b) total deformation

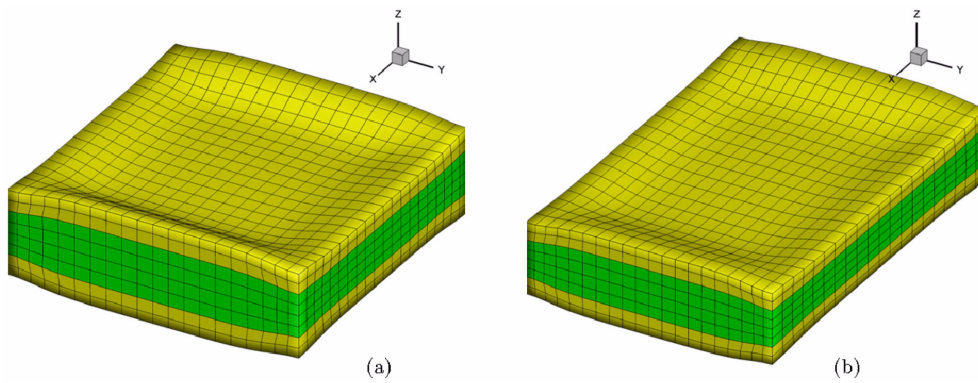


Fig. 10 Microscopic y_1 -tension deformations for unit cell II: (a) local fluctuating deformation, (b) total deformation

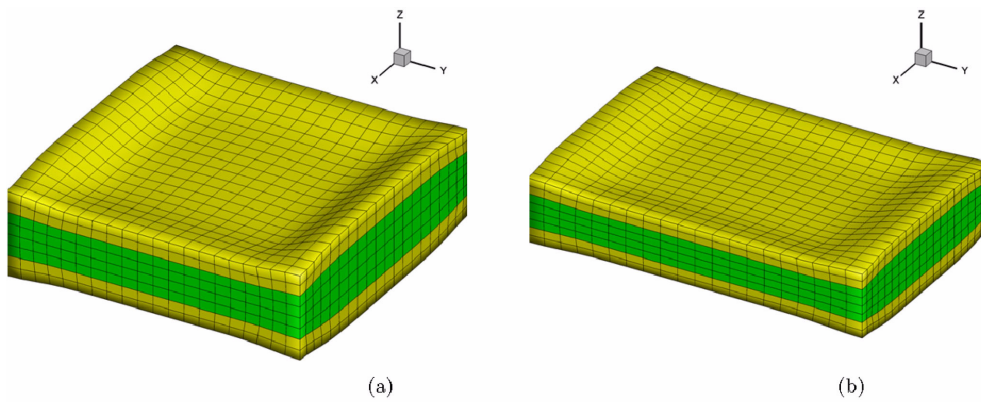


Fig. 11 Microscopic y_2 -tension deformations for unit cell II: (a) local fluctuating deformation, (b) total deformation

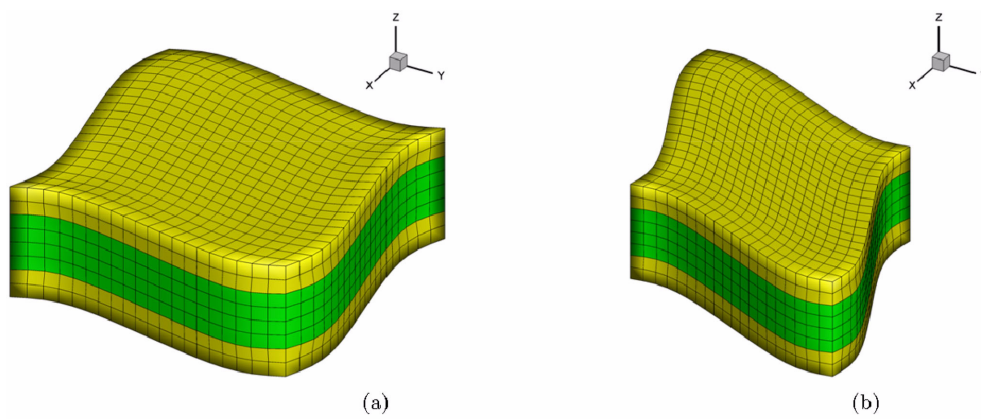


Fig. 12 Microscopic in-plane shear deformations for unit cell II: (a) local fluctuating deformation, (b) total deformation

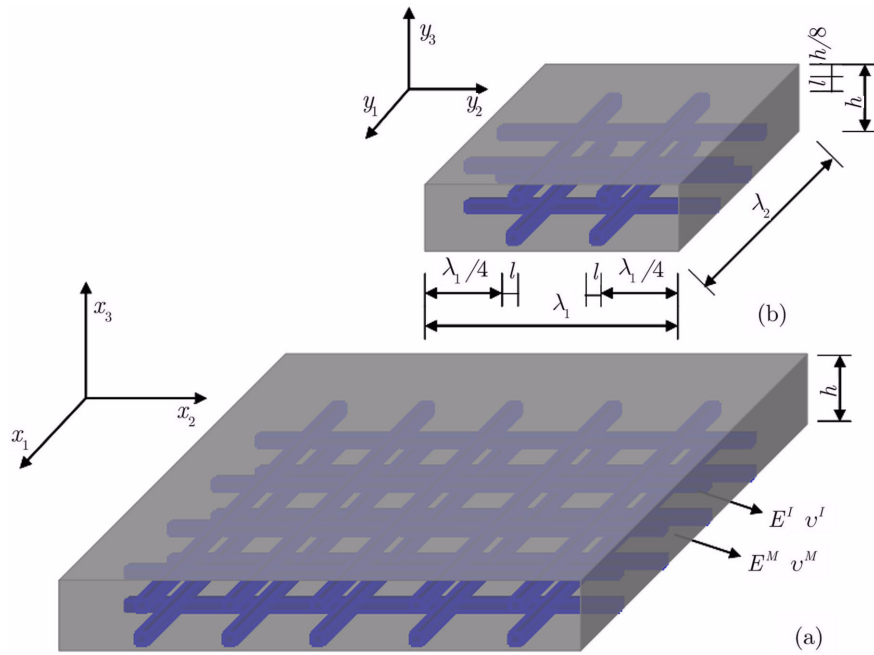


Fig. 13 Slab structure with two-layer reinforcement: (a) slab structure, (b) unit cell

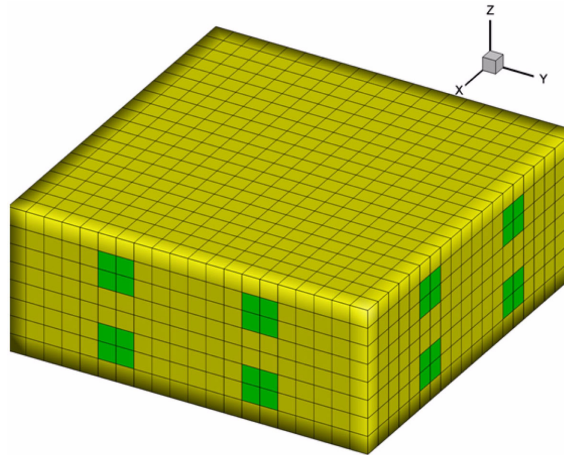


Fig. 14 Finite element unit cell discretization of the slab structure with two-layer reinforcement

4.3 Homogenization analysis for heterogeneous slab with two-layer reinforcement

In this sub-section the thin slab structure with two-layer fiber reinforcement as shown in Fig. 13 is considered. The geometric details of the selected unit cell are also listed in Fig. 13, where $l = 0.02m$ and this corresponds a volume fraction of 18% as well. The material properties are: $E^M = 10GPa$, $E^I = 100GPa$, $\nu_1 = \nu_2 = 0.3$. The unit cell finite element mesh for this problem is shown in Fig. 14. The local fluctuating deformations and total combined deformations

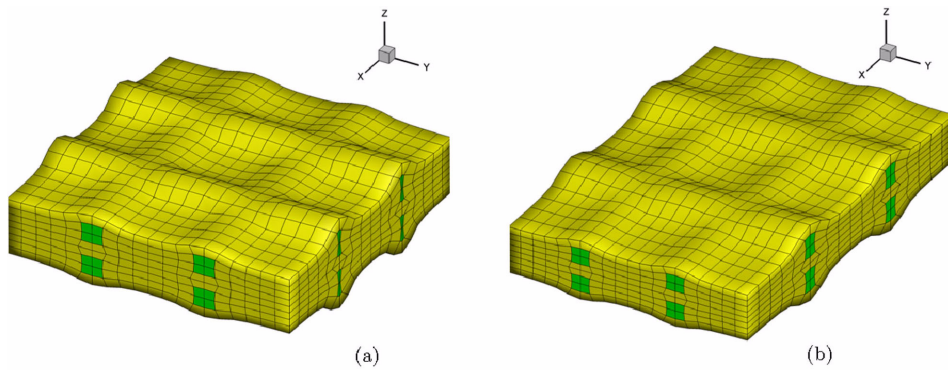


Fig. 15 Microscopic y_1 -tension deformations for unit cell of the slab structure with two-layer reinforcement: (a) local fluctuating deformation, (b) total deformation

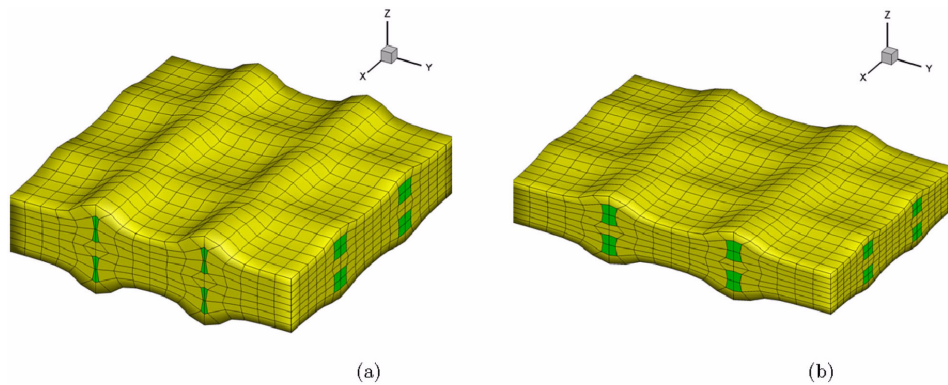


Fig. 16 Microscopic y_2 -tension deformations for unit cell of the slab structure with two-layer reinforcement: (a) local fluctuating deformation, (b) total deformation

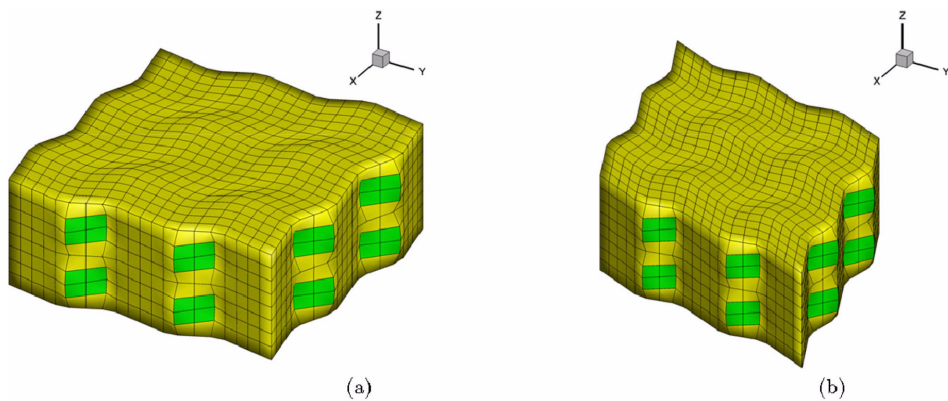


Fig. 17 Microscopic in-plane shear deformations for unit cell of the slab structure with two-layer reinforcement: (a) local fluctuating deformation, (b) total deformation

corresponding to the in-plane tension and shear modes are illustrated in Figs. 15-17. The homogenized material constants for this type of microstructure are given by

$$\mathbf{D}^{eff} = \begin{bmatrix} 2.2163 & 0.4975 & 0.0000 \\ 0.4975 & 2.2163 & 0.0000 \\ 0.0000 & 0.0000 & 0.5517 \end{bmatrix} \times 10GPa \quad (40)$$

A comparison between Eq. (39) and Eq. (40) shows that although these two kinds of inclusion have the same volume fraction but they yields different material properties due to the different characteristics of the microstructures.

4.4 Multiscale analysis of cantilever beam problem

The cantilever beam problem as shown in Fig. 18 is analyzed here to illustrate the proposed multiscale procedure. The cantilever beam is assumed to have the microstructure described in Fig. 2 with a thickness of $h = 0.08m$ and thus the homogenized material constants in Eq. (39) are employed for global structural analysis. Other geometric properties of the beam problem are taken as follows: length $L = 20m$, height $H = 4m$. The beam is subjected to a parabolic vertical traction with a total value of $P = 100KN$ at the free end. The uniform 20×4 finite element mesh as shown in Fig. 19 is used to solve the global homogenized problem under plane stress assumption and the stress results are plotted in Fig. 20. Subsequently the proposed multiscale method with unit cell analysis is used to extract the detailed local stress information. The corresponding local stress results at the four given locations, i.e., A, B, C, D points as indicated in Fig. 20 are clearly shown in Figs. 21-26, where in each figure the first row shows the unit cell stress distribution and the second row lists the stress solution of the half unit cell to gain a more clear looking at the stress distribution in the inclusions. The results in Figs. 21-26 evince that much higher stress occurs in the inclusion phase which can not be directly observed from the global structural analysis results as shown in Fig. 20.

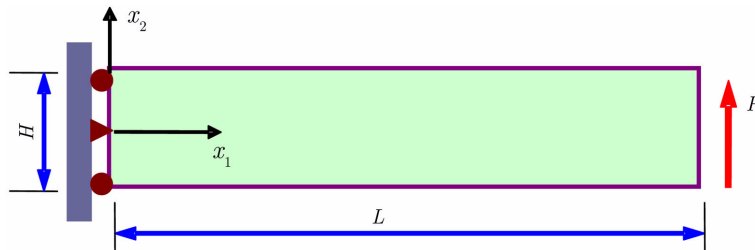


Fig. 18 Description of elastic cantilever beam problem

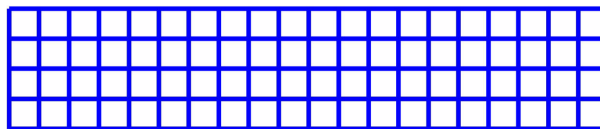


Fig. 19 Finite meshes for the cantilever beam problem

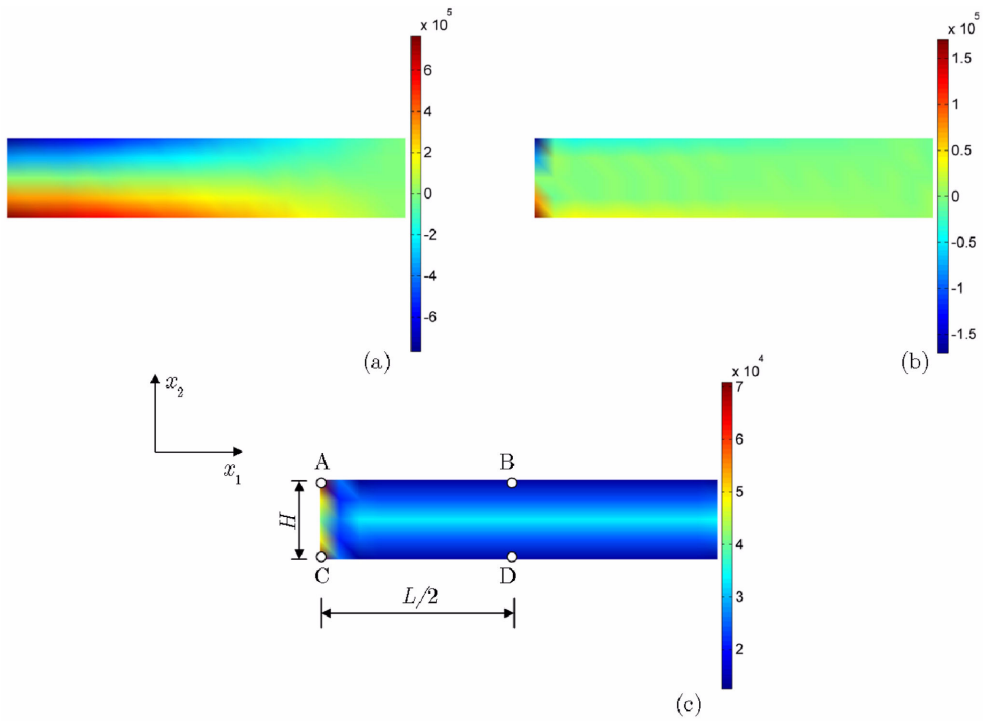


Fig. 20 Global stress distributions for the cantilever beam problem: (a) σ_{11} , (b) σ_{22} , (c) σ_{12}

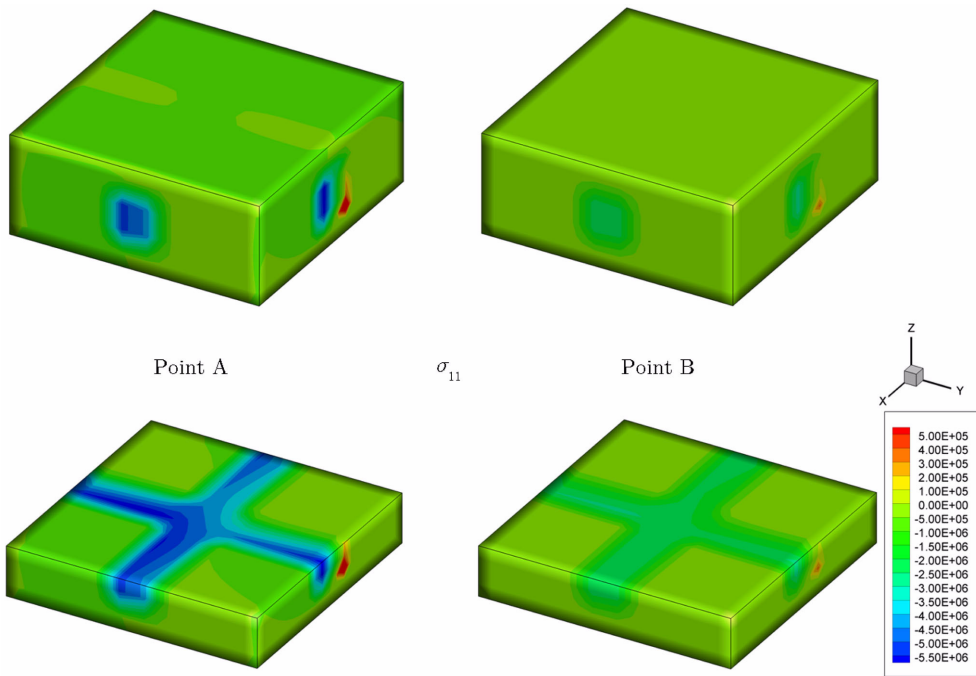


Fig. 21 Local unit cell stress distribution of σ_{11} at points A and B

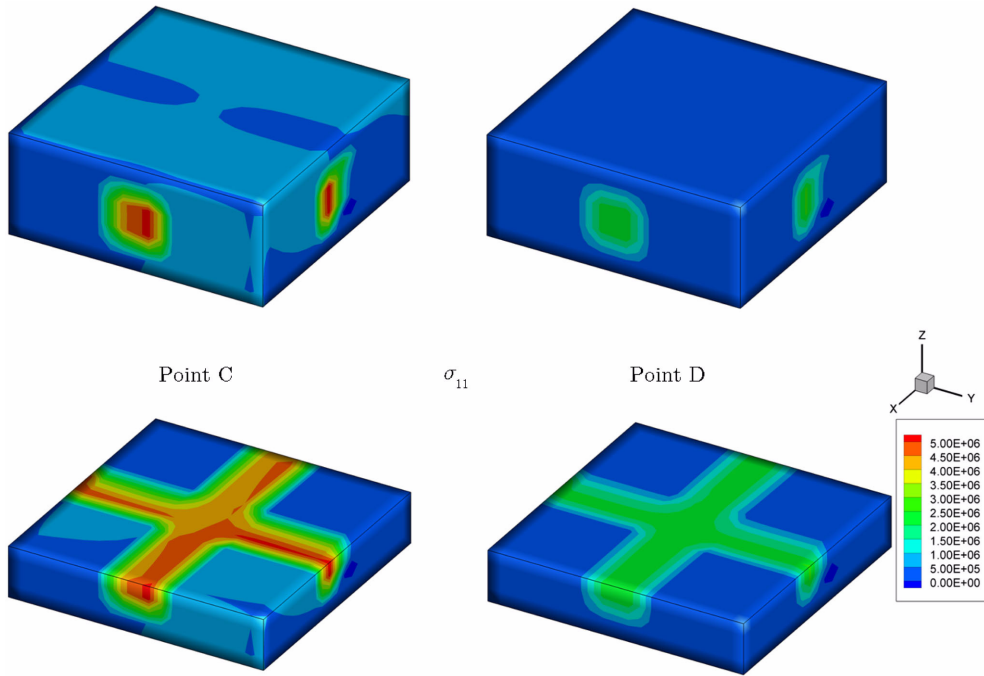


Fig. 22 Local unit cell stress distribution of σ_{11} at points C and D

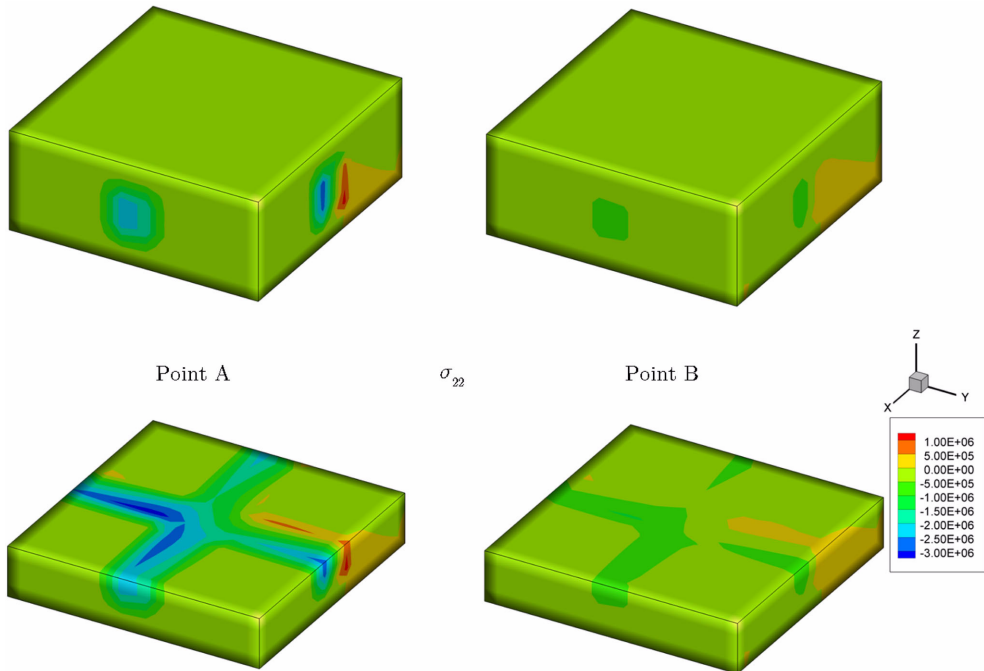


Fig. 23 Local unit cell stress distribution of σ_{22} at points A and B

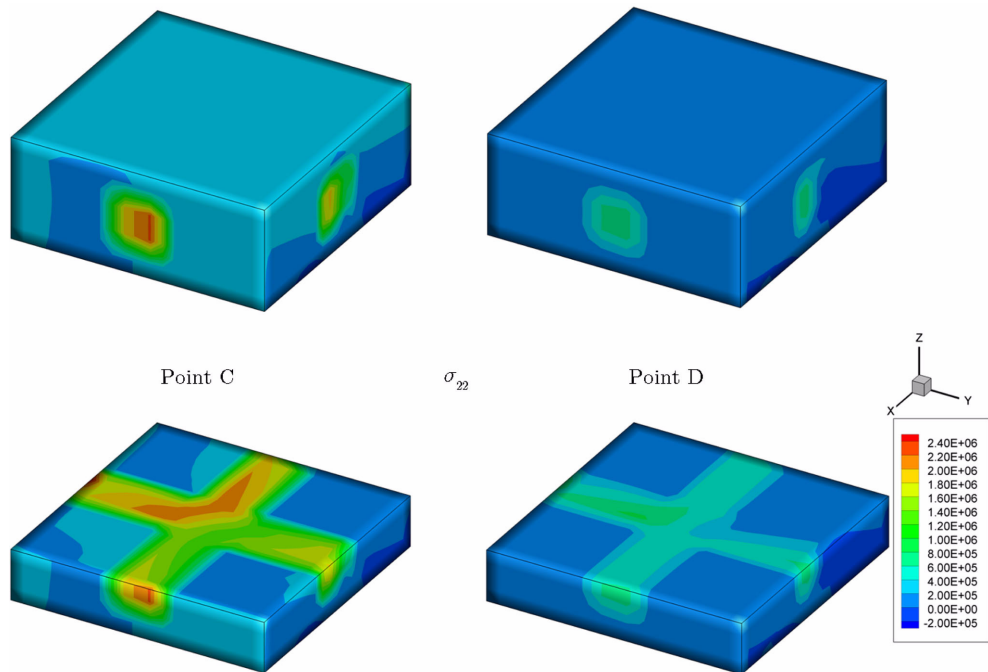


Fig. 24 Local unit cell stress distribution of σ_{22} at points C and D

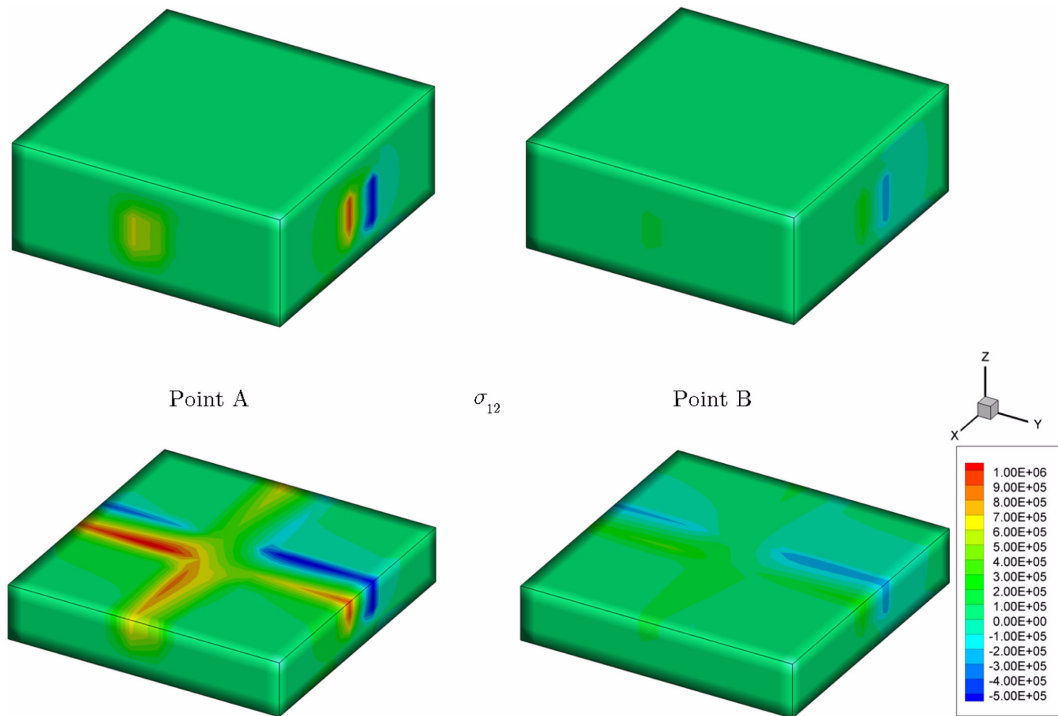


Fig. 25 Local unit cell stress distribution of σ_{12} at points A and B

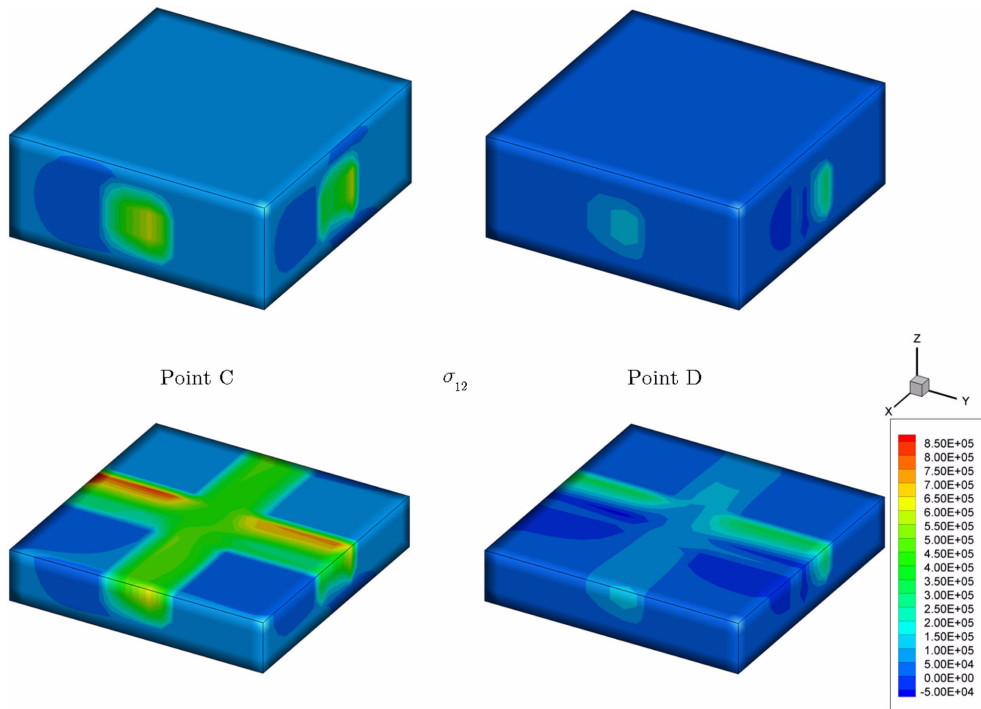


Fig. 26 Local unit cell stress distribution of σ_{12} at points C and D

5. Conclusions

An asymptotic expansion-based multiscale method was presented for analysis of thin slab or plate structures which have irreducible three dimensional structures. The proposed method adopted a special asymptotic expansion of the displacement field. The proposed asymptotic expansion of the displacement field takes into account the in-plane periodicity and yields a rational and clean formulation in which the thickness direction is treated globally. Thereafter the global and local problems were deduced in a very consistent manner under the asymptotic expansion theoretical framework. The global in-plane problem is the standard two dimensional plane stress problem while the local unit cell problem is completely three dimensional and it represents the physics of the slab structure, i.e., the thickness of the unit cell is the same as that of the structure. The local unit cell is subjected to periodic boundary conditions on the in-plane surfaces and the free surface conditions on the out of plane surfaces. Thereafter a variational formulation for the unit cell problem was presented where the free surface conditions are imposed naturally. Moreover the strain-controlled homogenization and the multiscale analysis procedure were discussed.

To verify the proposed method, an example with homogeneous materials was first analyzed through the present homogenization procedure and this led to a standard plan stress constitutive relationship as expected. Subsequently the homogenization analysis of a two-phase fiber reinforced slab structure was presented and the local fluctuating deformations and the combined total deformations were also shown in details. Meanwhile it was shown that different choices of unit cells yields identical homogenized material properties despite of the distinct local deformation

behaviors. Thereafter a two-layer reinforced slab structure that has the same volume fraction with the one-layer heterogeneous slab structure was studied and different material properties were observed due to the different characteristics of respective microstructures. Finally the proposed multiscale method was illustrated by solving a plane stress cantilever beam problem with heterogeneous microstructures.

Acknowledgements

The financial support of this work by the National Natural Science Foundation of China (10972188) and the Program for New Century Excellent Talents in University from China Education Ministry (NCET-09-0678) is gratefully acknowledged.

References

- Bensoussan, A., Lions, J.L. and Papanicolaou, G. (1978), *Asymptotic analysis for periodic Structures*, North-Holland Publishing Company, Amsterdam.
- Cao, L.Q., Cui, J.Z. and Zhu, D.C. (2002), "Multiscale asymptotic analysis and numerical simulation for the second order Helmholtz equation with oscillating coefficients over general convex domains", *SIAM J. Numer. Anal.*, **40**, 543-577.
- Chen, J.S. and Mehraeen, S. (2004), "Variationally consistent multiscale modeling and homogenization of stressed grain growth", *Comput. Method. Appl. M.*, **193**, 1825-1848.
- Chen, J.S. and Mehraeen, S. (2005), "Multi-scale modeling of heterogeneous materials with fixed and evolving microstructures", *Model. Simul. Mater. Sci.*, **13**, 95-121.
- Chung, P.W. and Namburu R.R. (2003), "On a formulation for a multiscale atomistic-continuum homogenization method", *Int. J. Solids Struct.*, **40**, 2563-2588.
- Fish, J. (eds) (2008), *Bridging the scales in science and engineering*, Oxford University Press.
- Fish, J., Shek, K., Pandheeradi, M. and Shephard M.S. (1997), "Computational plasticity for composite structures based on mathematical homogenization: theory and practice", *Comput. Method. Appl. M.*, **148**, 53-73.
- Ghosh, S. and Moorthy, S. (1995), "Elastic-plastic analysis of arbitrary heterogeneous materials with the voronoi cell finite element method", *Comput. Method. Appl. M.*, **121**, 373-409.
- Ghosh, S., Dakshinamurthy, V., Hu, C. and Bai, J. (2009), "A multi-scale framework for characterization and modeling ductile fracture in heterogeneous aluminum alloys", *J. Multiscale Model.*, **1**, 21-55.
- Guedes, J.S. and Kikuchi, N. (1989), "Preprocessing and postprocessing for materials based on the homogenization method with adaptive finite element methods", *Comput. Method. Appl. M.*, **83**, 143-198.
- Han, F., Cui, J.Z. and Yu, Y. (2008), "The statistical two-order and two-scale method for predicting the mechanics parameters of core-shell particle-filled polymer composites", *Interact. Multiscale Mech.*, **1**, 231-250.
- Hassani, B. and Hinton, E. (1998), *Homogenization and structural topology optimization*, Springer, Berlin.
- Hughes, T.J.R., *The finite element method: linear static and dynamic finite element analysis*, Dover publications: Mineola, NY, 2000.
- Kaczmarczyk, L., Pearce, C.J. and Bicanic, N. (2008), "Scale transition and enforcement of RVE boundary conditions in second-order computational homogenization", *Int. J. Numer. Method. Eng.*, **74**, 506-522.
- Mang, H.A., Aigner, E., Eberhardsteiner, J., Hackspiel, C., Hellmich, C., Hofstetter, K., Lackner, R., Pichler, B., Scheiner, S. and Stürzenbecher, R. (2009), "Computational multiscale analysis in civil engineering", *Interact. Multiscale Mech.*, **2**, 109-128.
- Mehraeen, S., Chen, J.S. and Hu, W. (2009), "An iterative asymptotic expansion method for elliptic eigenvalue problems with oscillating coefficients", *Comput. Mech.*, **46**, 349-361.
- Miehe, C. and Koch, A. (2002), "Computational micro-to-macro transitions of discretized microstructures

- undergoing small strains”, *Arch. Appl. Mech.*, **72**, 300-317.
- Mura, T. (1987), *Mechanics of defects in solids*, Nijhoff, The Hague.
- Nemat-Nasser, S. and Hori, M. (1993), *Micromechanics: Overall properties of heterogeneous materials*, Elsevier, Amsterdam.
- Ponte Castaneda, P. and Suquet, P. (1998), “Nonlinear composites”, *Adv. Appl. Mech.*, **34**, 171-303.
- Sanchez-Palencia, E. and Zaoui, A. (eds) (1987), *Homogenization techniques for composite media*, Springer, Berlin.
- Swan, C.C. (1994), “Techniques for stress- and strain-controlled homogenization of inelastic periodic composites”, *Interact. Multiscale Mech.*, **117**, 249-267.
- Takano, N., Ohnishi, Y., Zako, M. and Nishiyabu, K. (2000), “The formulation of homogenization method applied to large deformation problem for composite materials”, *Int. J. Solids Struct.*, **37**, 6517-6535.
- Wang, D., Chen, J.S. and Sun, L.Z. (2003), “Homogenization of magnetostrictive particle-filled elastomers using an interface-enriched reproducing kernel particle method”, *Finite Elem. Anal. Des.*, **39**, 765-782.
- Wu, C.T. and Koishi, M. (2009), “A meshfree procedure for the microscopic analysis of particle-reinforced rubber compounds”, *Interact. Multiscale Mech.*, **2**, 147-169.
- Yuan, Z. and Fish, J. (2009), “Hierarchical model reduction at multiple scales”, *Int. J. Numer. Method. Eng.*, **79**, 314-339.
- Zhang, H.W., Zhang, S., Bi, J.Y. and Schrefler, B.A. (2006), “Thermo-mechanical analysis of periodic multiphase materials by a multiscale asymptotic homogenization approach”, *Int. J. Numer. Method. Eng.*, **69**, 87-113.
- Zhang, X., Mehraeen, S., Chen, J.S. and Ghoniem, N. (2006), “Multiscale total Lagrangian formulation for modeling dislocation-induced plastic deformation in polycrystalline materials”, *Int. J. Multiscale Comput. Eng.*, **4**, 29-46.